Modulation-Noise-Free Continuously Tunable Single-Frequency CW Ti:Sapphire Laser With Intracavity-Locked Birefringent Etalon

Pixian Jin, Yongjie Xie, Xuechen Cao, Jing Su, Huadong Lu, and Kunchi Peng

***Abstract*— We present a continuously tunable single-frequency continuous wave (CW) Ti:Sapphire (Ti:S) laser with modulation-free-locked intracavity lithium niobate ($LiNbO_3$) birefringent etalon (BE), which is implemented by detecting the polarization state variation of the reflected laser beam from the BE. After the BE is stably locked, the continuous frequency-scanning range up to 40 GHz is obtained within the tuning range of 300 nm while the resonator length of the Ti:S laser is continuously scanned. Because the modulation signal is unnecessary in the presented Ti:S laser system, the influences of the extra modulation signal on the intensity noise as well as the frequency noise of the laser are thoroughly eliminated and the modulation-noise-free continuously tunable single-frequency CW Ti:S laser is successfully attained.**

***Index Terms*— Ti:S laser, birefringent etalon, modulation-free locking, noise.**

I. Introduction

ALL-SOLID-STATE continuous wave (CW) single-frequency tunable Ti:Sapphire (Ti:S) lasers have been applied in many fields including quantum optics and information [1], cold atom physics [2], quantum precision measurement [3], high-resolution spectroscopy [4] and so on, owing to their inherent excellent characteristics of high stability, low intensity noise, good beam quality, and broad output spectrum of 700-1000 nm [5], [6]. Especially, in order to satisfy the requirements of atomic physics, the output wavelengths of the Ti:S lasers are required to be continuously varied to exactly match the absorption lines of the atoms. For a single-frequency Ti:S laser, an etalon is often inserted into the ring resonator to keep single-longitude-mode (SLM) operation of laser. Meanwhile, the frequency-tuning of the laser can also be implemented by changing the effective optical path of the intracavity etalon (IE). In this tuning process, the laser frequency jumps step by step and one jump step corresponds to the free spectral range (FSR) of the laser resonator, owing to the oscillating laser mode hops one by one with the variation of the etalon's effective optical path. In order to realize the continuous frequency tuning of the laser, its cavity length should be continuously scanned. Due to the mode competition of the laser, the continuous frequency tuning can only be realized within one FSR of the laser resonator, generally several hundred megahertz, decided by the cavity length. However, for the atom-based applications, the Ti:S lasers with mode-hop-free tuning range of larger than several or dozens of gigahertz are required. To this end, the most common means is to lock the transmission peak of the IE onto the oscillating mode, so that the transmission peak of IE can shift with the sliding of laser mode when the laser cavity length is scanned. Then the continuous mode-hop-free tuning of the laser with a range larger than dozens of gigahertz can be realized [7]–[9]. A piezoelectric transducer-driven (PZT-driven) IE is the most popular candidate and often employed to achieve this goal [10]. However, in the PZT-based locking systems, in order to generate sufficient modulation depth with small modulation signals and then obtain well-defined error signals, the frequencies of the modulation signals have to correspond to the mechanical resonant frequencies of the used PZTs, which easily introduces the extra laser intensity noise at the corresponding frequencies, generally in dozens of kilohertz region. The increased intensity noise spike restricts the bandwidth and gain of feedback circuit used to reduce the background intensity noise of the laser that higher than shot noise limit (SNL), which increases the difficulty of the laser intensity noise reduction [11] and broadband squeezed light establishment [12]–[14] at lower frequency range covering dozens of kilohertz region. For the establishment of a broadband squeezed state with higher squeezing degree in low frequency band, the modulation noise spike should be eliminated. In 2017, our group adopted an electro-optic etalon to realize the continuous frequency tuning of the Ti:S laser, where the modulation signal was supplied to the etalon via the electro-optic effect of the crystal [15]. Although the frequency of the modulation signal could be selected arbitrarily and the intensity noise of the laser could be manipulated by changing the modulation signal's frequency to keep away from the relevant frequency ranges, the modulation signal still existed and influenced the downstream experimental system. In addition, it is well known that the modulation signal can also increase the frequency noise of the laser, which will enhance the difficulty to narrow the laser line width. Another way to accomplish the continuous frequency tuning of the Ti:S laser is based on the intracavity nonlinear loss deliberately introduced by a nonlinear crystal. With the inhibiting ability of the

Manuscript received September 29, 2021; revised November 23, 2021 and December 14, 2021; accepted December 17, 2021. Date of publication December 23, 2021; date of current version January 10, 2022. This work was supported in part by the National Natural Science Foundation of China under Grant 62105192, Grant 61975100, and Grant 62027821; in part by the Applied Basic Research Program of Shanxi Province under Grant 201901D211186; in part by the Program for the Innovative Talents of High Education Institutions of Shanxi; and in part by the Fund for Shanxi "1331 Project" Key Subjects Construction. *(Corresponding author: Huadong Lu.)*

The authors are with the State Key Laboratory of Quantum Optics and Quantum Optics Devices, Collaborative Innovation Center of Extreme Optics, Institute of Optoelectronics, Shanxi University, Taiyuan, Shanxi 030006, China (e-mail: pxjin@sxu.edu.cn; 18810891819@163.com; cao_xuechen@163.com; jingsu@sxu.edu.cn; luhuadong@sxu.edu.cn; kcpeng@sxu.edu.cn).

Color versions of one or more figures in this article are available at https://doi.org/10.1109/JQE.2021.3137832.

Digital Object Identifier 10.1109/JQE.2021.3137832

nonlinear loss to intracavity non-lasing mode [16], the output frequency of the Ti:S laser can be continuously tuned within a certain limit. Based on the presented method, our group successfully obtained a continuously tunable Ti:S laser with frequency scanning range up to 48 GHz in 2014 [17]. Because the nonlinear loss was introduced and the modulation locking system was eliminated, the intensity noise of the Ti:S laser was effectively suppressed. Nevertheless, the tuning range of the laser was decided by the nonlinear frequency-doubling conversion efficiency [17] which is dependent on the phase-matching of the nonlinear crystal, so it was limited by the phase matching bandwidth of the nonlinear crystal and could only be attained near a certain wavelength. For the purpose of realizing continuously tunable Ti:S laser covering broad range and satisfying many atom-based applications of quantum information and precise measurement, a modulation-free IE locking method is necessary to be employed to eliminate the influence of the extra modulation signal on the noise of the CW single-frequency tunable Ti:S laser.

In 1980, T. W. Hänsch and B. Couillaud stabilized a laser frequency by analyzing the polarization spectroscopy of the reflected light from a reference cavity and without any need for modulation technique [18]. On this basis, K. S. Gardner *et al.* first realized the stable single-frequency operation of a semiconductor laser in 2004 by utilizing an intracavity stabilized birefringent etalon (BE), where modulation signal was not necessary and the locking signal was obtained by analyzing the polarization of the reflection from the etalon [19], [20]. In this letter, in order to realize a modulation-noise-free and continuously tunable Ti:S laser, a BE made by lithium niobate ($LiNbO_3$) crystal is adopted in the laser resonator. With the assistance of the birefringent effect of the BE, the etalon was firstly locked to the oscillating laser mode to realize stable single-frequency operation of the laser by detecting the polarization state variation of the reflected laser from the BE. On this basis, a modulation-noise-free single-frequency CW Ti:S laser with the continuous frequency-tuning range larger than 40 GHz at the whole tuning range of 700-1000 nm is achieved in the experiment.

II. Experiment Setup

The experimental setup of the designed all-solid-state tunable single-frequency CW Ti:S laser with intracavity locked BE was illustrated in Fig. 1. The pump source was a home-made CW high power single-frequency 532 nm laser with the maximal output power of 14 W and stability better than ±0.4%(8h) [21]. The laser beam output from the pump source was collimated and focused to a 40 μm radius pump spot via lenses f_1 (f = 200 mm) and f_2 (f = 100mm), respectively, and used to pump the Ti:S crystal. The polarization of the pump laser was aligned by a half-wave plate in front of laser resonator to satisfy the requirement of the Ti:S crystal. The laser resonator was a bow-tie ring cavity formed by two concave mirrors with curve radius of 100 mm (M_1 and M_2) and two plane mirrors (M_3 and M_4). The input mirror of M_1 was coated with high-reflection (HR) film at 680-1030 nm and antireflection film at 532 nm. The concave mirror M_2 and plane mirror M_3 was coated with HR film at 680-1030 nm. The output coupler M_4 was coated with partial transmission film at 680-1030 nm with the transmissivity of 5.5%. The mirror M_3 was mounted on a long piezoelectric transducer (PZT,

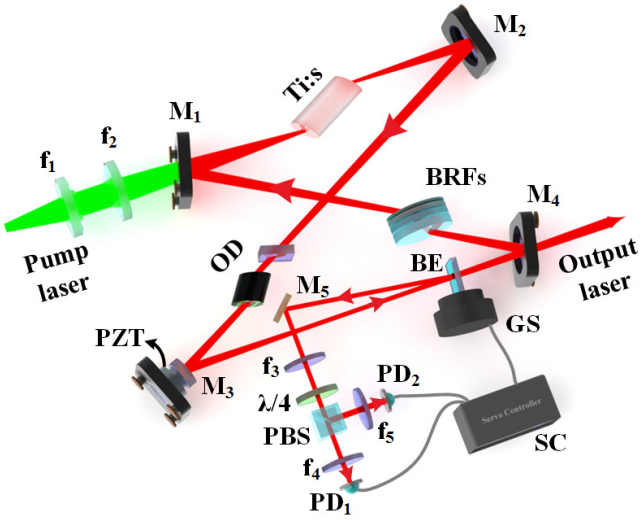

Fig. 1. Experimental setup of the continuous frequency-tuning laser with intravity-locked BE. Ti:S, Ti:Sapphire; OD, optical diode; BRFs, birefringent filters; BE, birefringent etalon; GS, galvanometer scanner; SC, servo controller; PZT, piezoelectric transducer; PBS, polarization beam splitter; PD_1-PD_2, photodetectors; M_1-M_5, mirrors; f_1-f_5, lenses.

HPSt150/14-10/25, Piezomechanik GmbH) to continuously scan the cavity length of the resonator by scanning the voltage loaded on the PZT. The gain medium of a Brewster-angle-cut Ti:S crystal with the doping concentration of 0.05 wt.% and size of Φ4mm × 20mm was placed between the mirrors of M_1 and M_2 and cooled by circulating cooling water. To ensure the unidirectional operation of the laser, the broad bandwidth optical diode consisting of a terbium gallium garnet (TGG) crystal surrounded by a permanent magnet and a thin quartz plate was adopted. The four-plate birefringent filters (BRFs) inserted into the resonator with its Brewster incident angle of 57° was utilized as coarse selector and tuning element. The thickness of BRFs was designed as 0.5 mm: 1 mm: 2.5 mm: 4.5 mm, and the angle of the optical axis was designed as 29.4° relative to its surfaces to achieve the tuning range of the laser broader than 300 nm [22]. In order to compensate the astigmatism induced by intracavity optical elements including Ti:S crystal, OD and BRFs, the folding angles of the concave mirrors M_1 and M_2 were set to 15.8°.

For the purpose of achieving modulation-free locking of IE and implementing continuous frequency tuning of the Ti:S laser, an etalon made of birefringent crystal ($LiNbO_3$ crystal) with thick of 1 mm was chosen as the intracavity fine selector as shown in Fig. 2. The optical axis of the crystal was in the direction of z-axis. Its incident and transmission surfaces were in x-o-z plane and these two parallel surfaces were both uncoated and polished. The etalon was adhered to the rotation axis of the galvanometer scanner (GS, 6220HM40BR, Cambridge Technology), with the rotation axis along x-axis, to control its incidental angle. Then, the etalon was inserted into the resonator with its x-axis setting about 2∼3 degree relative to the polarization orientation of the oscillating light. Thus, the incident laser (E_0) would decompose into two components in the crystal, the major one E_1 and the minor one E_2. The polarization orientations of E_1 and E_2 were in the x- and z-axis directions of the crystal, respectively. According to the birefrengence and reflection properties of the etalon,

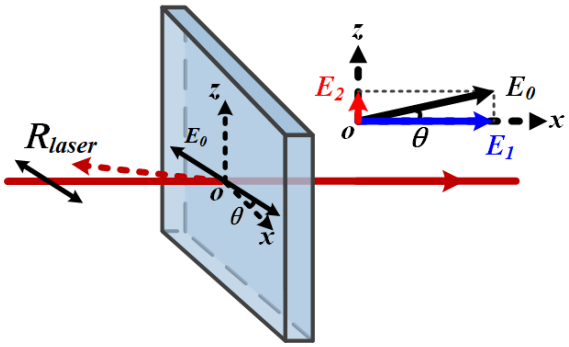

Fig. 2. Structure chart of the BE.

the polarization property of the reflected laser from the etalon (R_{laser}) was varied when the laser frequency resonated with the etalon or not, as analyzed in Ref. [19]. When the major one laser component E_1 was resonant with the etalon, its reflection coefficient equaled zero, and the reflected laser was linearly polarized along z-axis (only E_2 component could be reflected). However, when it was mismatched with the etalon, the reflected laser was elliptically polarized with different helicity. By detecting this polarization state variation, the deviation between the laser frequency and etalon's resonance frequency could be extracted and used as the ES for feedback to lock the etalon with the oscillating mode [18], [19]. On this basis, the reflected laser beam from the etalon was separated from the main optical path by rotating the etalon with a small tilt angle in the vertical direction of the light and guided by mirror M_5 to pass through the discriminator consisting of a quarter-wave plate and a PBS. Then, the reflected laser was split into two parts and detected by a pair of photodetectors (PD_1 and PD_2) to extract the ES in the homemade servo controller (SC). The lenses f_3, f_4 and f_5 ensured that the reflected laser could be always focused into the photodetectors in the process of rotating the incidental angle of the etalon by controlling the voltage of GS.

III. Experiment Results and Analysis

When the laser was working at the wavelength of 795 nm, the output power of the laser versus the pump power was recorded by a power meter (PM30, Coherent Co., Ltd.) and shown in Fig. 3. The maximal output power of 1.95 W at the pump power of 11.4 W was obtained with the slope efficiency of 25%. The power fluctuation of the laser working at maximal output power was recorded over 3.5 h with the sample rate of 1 sample per second and the corresponding fluctuation was less than 0.29% (rms value) as shown in Fig. 4. The laser power fluctuation could be further reduced by improving the pump power stability, assembling the whole laser system in a temperature controlled environment, and even feedback controlling the deliberately introduced nonlinear loss in the resonator [23]. The spatial profile of the output laser beam was measured by a beam quality meter (M2SETVIS, Thorlabs) and depicted in inset of the Fig. 3. The measured M^2 values of the laser beam were 1.05 and 1.10 in x and y directions, respectively. The longitudinal mode structure of the laser was also monitored by a scanned confocal Fabry-Perot interferometer (FPI) and the single-longitudinal-mode

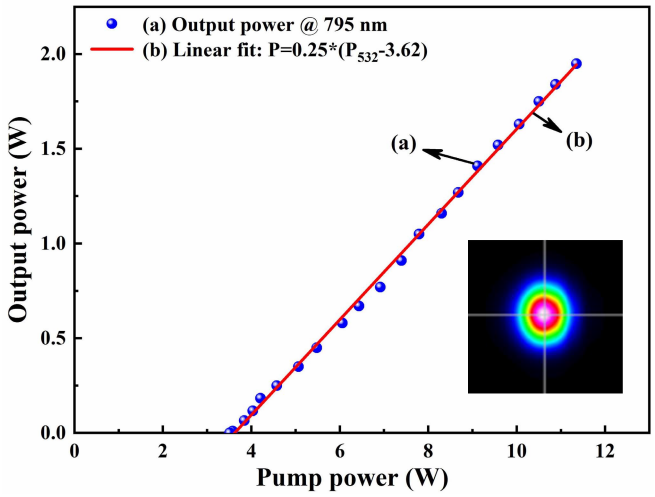

Fig. 3. Output power of the 795 nm laser versus the pump power. Inset: spatial beam profile of output laser.

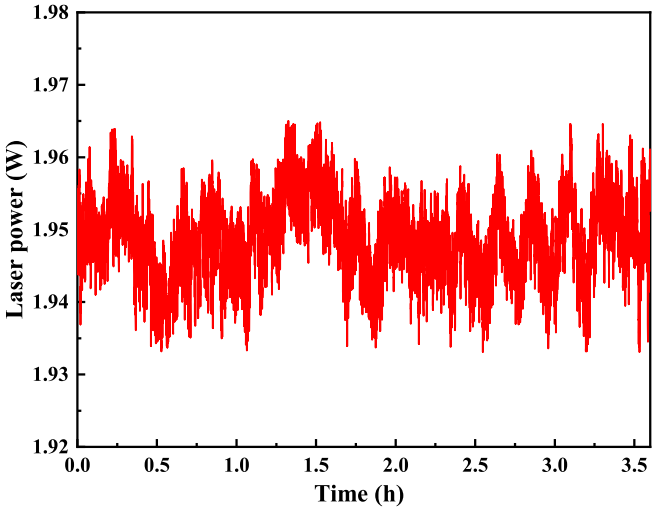

Fig. 4. Power stability of 795 nm laser over 3.5 hours.

operation of the laser was observed in experiment. By rotating the BRFs along its normal axis, the output wavelength of the laser could be tuned from 692 nm to 995 nm, and the attained tuning range of the laser was broader than 300 nm [22]. The output powers at the typical wavelengths of 766 nm, 770 nm, 780 nm, 852 nm and 895 nm were 2.2 W, 2.4 W, 2.1 W, 2.15 W and 1.8 W, respectively. Further, only by varying the incident angle of the etalon, the output wavelength of the laser could be finely tuned within 0.12 nm (58 GHz, one FSR of the adopted etalon) with the tuning precision corresponding to one FSR of the resonator, about 600 MHz.

To implement the continuous frequency-tuning of the Ti:S laser, the transmission peak of the intracavity etalon had to be locked to the oscillating mode of the laser resonator. To this end, both detected direct current (DC) signals from PD_1 and PD_2 were added ($I_1 + I_2$) and subtracted (I_1-I_2) in SC, respectively, to extract the ES by means of the operation of (I_1-I_2)/($I_1 + I_2$) [19]. The extracted ES was firstly observed in experiment by scanning the incident angle of the etalon.

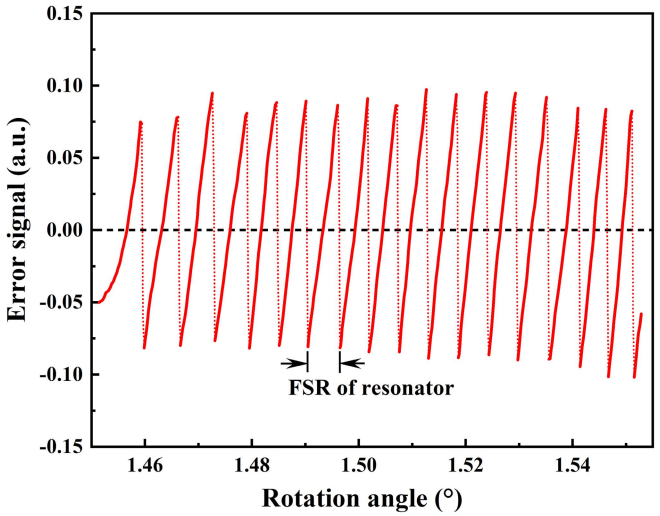

Fig. 5. Experimentally measured ES by rotating the incident angle of BE.

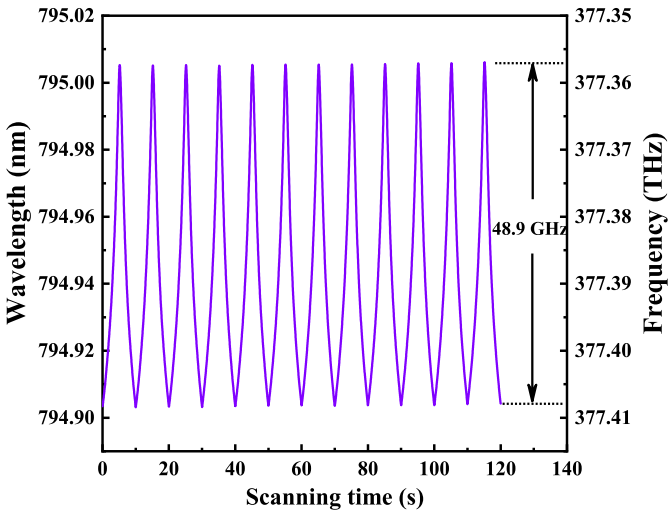

Fig. 6. Wavelengths observed while scanning the cavity length of the laser.

The observed ES was shown in Fig. 5. The experimental result presented a zero-crossing saw-tooth signal owing to the lasing modes hopped one by one when the incident angle of the etalon was rotated and the period of the signal corresponded to the FSR of the laser resonator with the value of 600 MHz, which could be well used to lock the etalon with the oscillating mode of the laser and realize continuous frequency tuning of the laser with broad tuning range. Then the error signal was amplified and integrated with integral time of about 1 millisecond in the homemade SC to obtain the control signal. Lastly, the generated control signal was loaded onto the GS to feedback control the incidental angle of the etalon, and consequently the etalon was successfully locked to the oscillating mode of the laser. After the BE was locked to the oscillating wavelength near 795 nm and the cavity length of the laser was continuously scanned by applying a high-voltage scanning signal with period of 10 s onto the PZT adhered to the M_3, the mode-hop-free tuning of the laser with the range up to 48.9 GHz was realized, as shown in Fig. 6, which was measured and recorded by a wavelength meter (WS6/765, High Finesse Laser and Electronic System) with the measurement resolution of 0.1 pm (50 MHz) and the sample rate of 100 samples per second. The nonlinear variation of the output wavelength with scanning time resulted from the nonlinearity of the PZT. When the intracavity BE was locked to the oscillating wavelengths of 720 nm, 780 nm, 852 nm and 960 nm by adjusting the BRFs, the continuous frequency-tuning ranges of 45.4 GHz, 44.8 GHz, 46.7 GHz and 43.2 GHz were attained, respectively, which meant that the output frequency of the laser could be continuously scanned at any wavelengths within the broad tuning range. The laser power fluctuations were less than 10% in the continuous frequency tuning processes.

Besides, in order to further demonstrate the superiority of the presented modulation-free etalon-locking method, the influence of the etalon-locking system on the laser intensity noise was investigated. The intensity noise of the laser relative to the SNL was measured by a homemade low-noise homodyne detector with the measurement bandwidth from 10 kHz to 5 MHz and analyzed by a spectrum analyzer with the resolution bandwidth (RBW) of 510 Hz and the video bandwidth (VBW) of 100 Hz. The measured results of the present Ti:S laser with BE and the traditional Ti:S lasers with PZT-driven and electro-optic etalons were compared and shown in Fig. 7. The frequency of the modulation signal for the PZT-driven etalon was 26.9 kHz, which was matching with the mechanical resonant frequency of the used PZT, and the corresponding laser intensity noise was shown as red curve (a) in Fig. 7. While the frequencies of the modulation signals for the electro-optic etalon were discretionarily chosen as 50 kHz and 130 kHz, and the corresponding laser intensity noises were shown as blue (b) and green (c) curves, respectively, in Fig. 7. The intensity noise spectrum of the Ti:S laser based on the modulation-free BE was depicted as black curve (d) in Fig. 7. It could be obviously found that the modulation noises imprinted in the intensity noise spectrum of the Ti:S laser and the intensity noises were both dramatically increased at the analysis frequencies corresponding to the modulation frequencies and their second harmonics in the laser system. However, when the BE was adopted in the Ti:S laser and locked by means of modulation-free locking, there was not any extra noises in the laser intensity noise spectrum, which directly confirmed that the influence of the extra modulation signal on the intensity noise was completely eliminated in the continuously tunable Ti:S laser. The remaining broadband noise except the modulation noise below 2 MHz in the Fig. 7 was caused by the noise sources including pump noise, spontaneous-emission noise, dipole fluctuation noise, vacuum noise caused by output coupler and noise introduced by intracavity losses [24], [25].

Except for the influence on the intensity noise of the continuously tunable Ti:S laser, the extra modulation signal also affected the frequency noise of the laser. The frequency noise properties of the Ti:S lasers with the present BE and traditional electro-optic etalon with modulation frequency of 50 kHz were experimentally investigated. A confocal FPI with the FSR of 750 MHz and fineness of 10 was adopted to measure the frequency noise of the laser [26], [27]. When the laser frequency was manually maintained close to the middle of the Fabry-Perot fringe, the transmitted signal of the FPI for 1 s

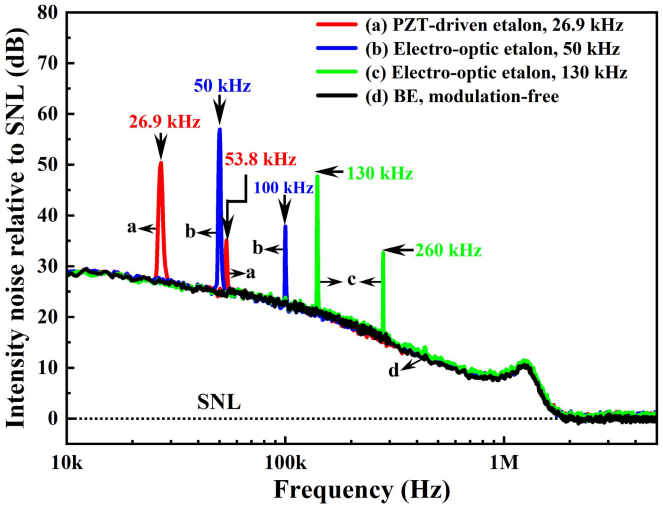

Fig. 7. Intensity noises of the Ti:S lasers with (a) PZT-driven etalon with the modulation frequency of 26.9 kHz, red curve; (b) electro-optic etalon with the modulation frequency of 50 kHz, blue curve; (c) electro-optic etalon with the modulation frequency of 130 kHz, green curve; (d) BE with modulation-free, black curve.

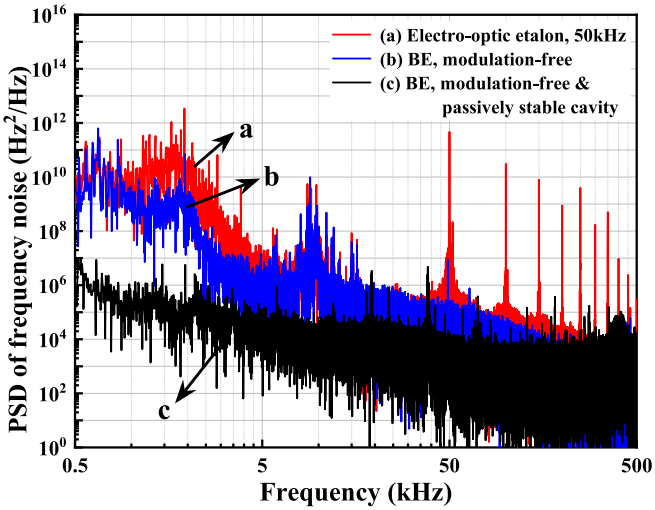

Fig. 8. Frequency noises of the Ti:S lasers with (a) electro-optic etalon with the modulation frequency of 50 kHz, red curve; (b) BE with modulation-free, blue curve; (c) BE with modulation-free and in a passively stable cavity, black curve.

with a sampling frequency of 2 MHz was recorded by a digital oscilloscope. The measured data were analyzed by fast Fourier transform (FFT) and the power spectral densities (PSD) of the frequency noises were obtained. In order to easily illustrate the comparison results of the influence of the modulation signal on the laser frequency noise, the obtained PSD of the frequency noises within the frequency range from 500 Hz to 500 kHz were plotted and shown in Fig. 8. The red curve in the figure showed the frequency noise of the Ti:S laser with electro-optic etalon with the modulation frequency of 50 kHz, and the blue curve showed that with modulation-free BE. From these curves, it can be found that, when the modulation signal existed in the laser system, the frequency noise of the laser at the analysis frequencies corresponding to the modulation frequency and its harmonic series were visibly increased. Furthermore, it was worth noting that the laser frequency noises at other frequency ranges were also relatively higher. This was attributed to the laser system was assembled by some separate optical elements in experiment so that the length of the laser cavity was susceptible to the ambient temperature drift, vibration and airflow. When the whole elements of the Ti:S laser resonator with BE were mounted in a stable monoblock construction with temperature control at the accuracy of 0.02 °C, the laser frequency noise was also measured in experiment as shown in Fig. 8 (black curve), which showed that the laser frequency noise was obviously reduced at the frequency range lower than 10 kHz. The frequency noise of the laser at 40 kHz, harmonic and sub-harmonic may be caused by the mechanical resonance of the mirror brackets, and that above 400 kHz may be caused by the measurement process.

The experiment results revealed that the influences of the extra modulation signal on the intensity as well as the frequency noises were both vanished once the BE and modulation-free locking method were adopted in the Ti:S laser. This was resulted from that, when the BE was utilized, the error signal used to lock it was extracted just by detecting the polarization variation of the reflected laser beam from it and the modulation signal that was necessary for traditional PZT-driven or electro-optic etalons locking was not introduced into the laser system. In this case, the laser intensity and frequency were not modulated, so there were no modulation noises imprinted in laser intensity and frequency noises.

IV. Conclusion

In summary, we presented a modulation-noise-free continuously tunable single-frequency CW Ti:S laser with the output power of about 2 W, which was implemented by feedback locking the intracavity $LiNbO_3$ BE with the modulation-free locking method. By setting the angle between the etalon's x-axis and the laser's polarization orientation as 2° ~3° and further detecting the polarization state variation of the reflected laser from the BE, the ES was successfully extracted and used to lock the BE to the oscillating wavelength of the resonator. After the intracavity BE was stably locked, the continuous frequency-tuning ranges up to 40 GHz at different operating wavelengths were both realized while the cavity length of the laser resonator was continuously scanned. Due to the modulation signal was unnecessary to lock the intracavity etalon in the presented continuously tunable Ti:S laser, the influences of the extra modulation signal on the intensity noise as well as the frequency noise were eliminated thoroughly. The obtained modulation-noise-free continuously tunable single-frequency CW Ti:S laser can be well used in the research fields of quantum-enhanced precision measurement, quantum information network and cold-atom physics.

References

[1] H. J. Kimble, "The quantum internet," *Nature*, vol. 453, pp. 1023–1030, Jun. 2008.

[2] T. Kuwamoto, K. Honda, Y. Takahashi, and T. Yabuzaki, "Magneto-optical trapping of Yb atoms using an intercombination transition," *Phys. Rev. A, Gen. Phys.*, vol. 60, no. 2, pp. R745–R748, Aug. 1999.

[3] B.-B. Li *et al.*, "Quantum enhanced optomechanical magnetometry," *Optica*, vol. 5, no. 7, pp. 850–856, 2018.

[4] W. Vassen, C. Zimmermann, R. Kallenbach, and T. W. Hänsch, "A frequency-stabilized titanium sapphire laser for high-resolution spectroscopy," *Opt. Commun.*, vol. 75, nos. 5–6, pp. 435–440, Mar. 1990.

[5] G. T. Maker and A. I. Ferguson, "Ti: Sapphire laser pumped by a frequency-doubled diode-pumped Nd: YLF laser," *Opt. Lett.*, vol. 15, pp. 375–377, Apr. 1990.

[6] Y. Sun, H. D. Lu, and J. Su, "Continuous-wave, single-frequency, all-solid-state Ti: Al_2O_3 laser," *Acta Sin. Quantum Opt.*, vol. 14, pp. 344–347, Apr. 2008.

[7] Accessed: Dec. 10, 2021. [Online]. Available: https://www.spectra-physics.com/f/matisse-2-tunable-ring-laser

[8] Accessed: Dec. 10, 2021. [Online]. Available: https://www.tekhnoscan.com/english/ring_lasers.htm

[9] Accessed: Dec. 10, 2021. [Online]. Available: https://www.m2lasers.com/solstis.html

[10] X. J. Sun, J. Wei, W. Z. Wang, and H. D. Lu, "Realization of a continuous frequency-tuning Ti: Sapphire laser with an intracavity locked etalon," *Chin. Opt. Lett.*, vol. 13, Jul. 2015, Art. no. 071401.

[11] L. Bai, X. Wen, Y. Yang, J. He, and J. Wang, "Laser intensity noise suppression for preparing audio-frequency squeezed vacuum state of light," *Appl. Sci.*, vol. 10, no. 4, p. 1415, Feb. 2020.

[12] X. Wen, Y. S. Han, J. Y. Liu, J. He, and J. M. Wang, "Polarization squeezing at the audio frequency band for the Rubidium D_1 line," *Opt. Exp.*, vol. 25, pp. 20737–20748, Aug. 2017.

[13] K. McKenzie, M. B. Gray, P. K. Lam, and D. E. McClelland, "Technical limitations to homodyne detection at audio frequencies," *Appl. Opt.*, vol. 46, pp. 3389–3395, Jun. 2007.

[14] M. S. Stefszky *et al.*, "Balanced homodyne detection of optical quantum states at audio-band frequencies and below," *Classical Quantum Gravity*, vol. 29, no. 14, Jul. 2012, Art. no. 145015.

[15] P. X. Jin, H. D. Lu, Y. X. Wei, J. Su, and K. C. Peng, "Single-frequency CW Ti: Sapphire laser with intensity noise manipulation and continuous frequency-tuning," *Opt. Lett.*, vol. 42, pp. 143–146, Jan. 2017.

[16] K. I. Martin, W. A. Clarkson, and D. C. Hanna, "Self-suppression of axial mode hopping by intracavity second-harmonic generation," *Opt. Lett.*, vol. 22, pp. 375–377, Mar. 1997.

[17] H. D. Lu, X. J. Sun, M. H. Wang, J. Su, and K. C. Peng, "Single frequency Ti: Sapphire laser with continuous frequency-tuning and low intensity noise by means of the additional intracavity nonlinear loss," *Opt. Exp.*, vol. 22, pp. 24551–24558, Oct. 2014.

[18] T. W. Hansch and B. Couillaud, "Laser frequency stabilization by polarization spectroscopy of a reflecting reference cavity," *Opt. Commun.*, vol. 35, no. 3, pp. 441–444, Dec. 1980.

[19] K. S. Gardner, R. H. Abram, and E. Riis, "A birefringent etalon as single-mode selector in a laser cavity," *Opt. Exp.*, vol. 12, pp. 2365–2370, May 2004.

[20] R. H. Abram, K. S. Gardner, E. Riis, and A. I. Ferguson, "Narrow linewidth operation of a tunable optically pumped semiconductor laser," *Opt. Exp.*, vol. 12, pp. 5434–5439, Nov. 2004.

[21] Y. J. Wang, Y. H. Zheng, Z. Shi, and K. C. Peng, "High-power single-frequency Nd: YVO_4 green laser by self-compensation of astigmatisms," *Laser Phys. Lett.*, vol. 9, pp. 506–510, Jun. 2012.

[22] J. Wei, X. C. Cao, P. X. Jin, J. Su, H. D. Lu, and K. C. Peng, "Diving angle optimization of BRF in a single-frequency continuous-wave wideband tunable titanium: Sapphire laser," *Opt. Exp.*, vol. 29, pp. 6714–6725, Mar. 2021.

[23] P. X. Jin, H. D. Lu, J. Su, and K. C. Peng, "Scheme for improving laser stability via feedback control of intracavity nonlinear loss," *Appl. Opt.*, vol. 55, pp. 3478–3482, May 2016.

[24] J. Belfi, J. Galli, G. Giusfredi, and F. Marin, "Intensity noise of an injection-locked Ti: Sapphire laser: Analysis of the phase-noise-to-amplitude-noise conversion," *J. Opt. Soc. Amer. B, Opt. Phys.*, vol. 23, pp. 1276–1286, Jul. 2006.

[25] H. D. Lu, J. Su, C. D. Xie, and K. C. Peng, "Experimental investigation about influences of longitudinal-mode structure of pumping source on a Ti: Sapphire laser," *Opt. Exp.*, vol. 19, pp. 1344–1353, Jan. 2011.

[26] O. Mhibik, T.-H. My, D. Paboeuf, F. Bretenaker, and C. Drag, "Frequency stabilization at the kilohertz level of a continuous intracavity frequency-doubled singly resonant optical parametric oscillator," *Opt. Lett.*, vol. 35, pp. 2364–2366, Jul. 2010.

[27] A. Ly, C. Siour, and F. Bretenaker, "30-Hz relative linewidth Watt output power 1.65 μm continuous-wave singly resonant optical parametric oscillator," *Opt. Exp.*, vol. 25, pp. 9049–9060, Apr. 2017.

Pixian Jin was born in 1989. He received the Ph.D. degree in laser technology from Shanxi University, Taiyuan, China, in 2018.

He is currently a Researcher in optics with the Institute of Optoelectronics, Shanxi University. His current research interests include all-solid-state laser technology and optoelectronic technology.

Yongjie Xie was born in 1997. She received the B.S. degree in the Internet of Things from the Beijing University of Technology, Beijing, China, in 2019. She is currently pursuing the master's degree in optical engineering with the Institute of Optoelectronics, Shanxi University.

Her current research interest is optoelectronic technology.

Xuechen Cao was born in 1996. He received the B.S. degree in applied physics from Shanxi Normal University, Taiyuan, China, in 2014. He is currently pursuing the master's degree in optics with the Institute of Optoelectronics, Shanxi University.

His current research interest is tunable optics devices.

Jing Su was born in 1979. She received the Ph.D. degree in physics from Nankai University, Tianjin, China, in 2007.

She is a currently a Professor with the Institute of Optoelectronics, Shanxi University. Her current research interests include all-solid-state laser technology, quantum optics devices, and tunable optics devices.

Huadong Lu was born in 1981. He received the Ph.D. degree in laser technology from Shanxi University, Taiyuan, China, in 2011.

He is a currently a Professor with the Institute of Optoelectronics, Shanxi University. His current research interests include all-solid-state laser technology, quantum optics devices, and tunable optics devices.

Kunchi Peng was born in 1936. He received the B.S. degree in physics from Sichuan University, Chengdu, China, in 1961.

He was a Visiting Scholar with Paris 11th University, Orsay, France, from 1980 to 1982; The University of Texas at Austin from 1982 to 1984; and the California Institute of Technology, Pasadena, from 1988 to 1989. He has been a Professor with the Institute of Optoelectronics, Shanxi University, Shanxi, China, since 1990. His current research interests include all-solid-state laser technology, quantum information networks, and quantum optics devices.

Prof. Peng was elected as a fellow of the Optical Society of America in April 2006 and is a member of the Chinese Physical Society.